

Nonequilibrium Response for Markov Jump Processes: Exact Results and Tight Bounds

Timur Aslyamov^{1,*} and Massimiliano Esposito^{1,†}

¹*Department of Physics and Materials Science, University of Luxembourg, L-1511 Luxembourg City, Luxembourg*
(Dated: August 9, 2023)

Generalizing response theory of open systems far from equilibrium is a central quest of nonequilibrium statistical physics. Using stochastic thermodynamics, we develop an algebraic method to study the response of nonequilibrium steady state to arbitrary perturbations. This allows us to derive explicit expressions for the response of edge currents as well as traffic to perturbations in kinetic barriers and driving forces. We also show that these responses satisfy very simple bounds. For the response to energy perturbations, we straightforwardly recover results obtained using nontrivial graph-theoretical methods.

Introduction.—Linear response theory is a central tenet in statistical physics [1–3]. The response of systems in steady state at, or close to, equilibrium is described by the seminal dissipation-fluctuation relation (DFR) [4, 5]. Generalizations to study the response of systems in nonequilibrium steady state (NESS) are a more recent endeavor, in particular since the advent of stochastic thermodynamics [6–16]. Understanding the response of far-from-equilibrium systems is of great conceptual but also practical importance (e.g. to characterize homeostasis, design resilient nanotechnologies, detect critical transitions, and metabolic control). Progress in this direction relies on our ability to derive useful expressions for NESS responses, and possibly derive practically meaningful bounds for them.

In this Letter, we study the NESS response of Markov jump processes within stochastic thermodynamics. In this context, Ref. [17] constitute a frontier. The authors studied the response to perturbations of the energy landscape parameters. They derived an exact result and two bounds using graph-theoretic methods, which can be quite tedious and nonintuitive to use [18–20]. We develop a novel approach based on simple linear algebra, which allows us to go significantly further than currently known results. We first derive a simple and elegant expression for the response of a NESS to arbitrary perturbations. We use it to straightforwardly reproduce the main result [17] for the NESS response to perturbations of the energy landscape. But more importantly we also use it to derive novel and simple expressions for the response of edge currents and traffic to kinetic barriers and driving forces perturbations. We furthermore derive four remarkably simple bounds for these four quantities (see Table I), which can be added to the list of simple bounds valid far-from-equilibrium, together with thermodynamic uncertainty relations [21, 22] and speed limits [23].

Setup.—We consider a Markov jump process over a discrete set of N states. Transitions between these states are described by the rate matrix \mathbb{W}/τ , where the element W_{nm}/τ defines the probability per unit time τ to jump from state m to state n . Below we choose $\tau = 1$, to adimensionalize the matrix \mathbb{W} . We assume that all transitions are reversible and that the matrix \mathbb{W} is irreducible [24]. This ensures the existence of a unique

steady-state probability distribution $\boldsymbol{\pi} = (\pi_1, \dots, \pi_N)^\top$ satisfying

$$\mathbb{W} \cdot \boldsymbol{\pi} = \mathbf{0}, \quad (1)$$

where the length of the vector $\boldsymbol{\pi}$ is $|\boldsymbol{\pi}| = 1$. When the rates depend on a model parameter η , one can define the linear response (resp. sensitivity) of the nonequilibrium state as $\partial_\eta q$ (resp. $\partial_\eta \ln q$) for an arbitrary quantity q .

General theory.—The rate matrix \mathbb{W} in Eq. (1) has only one zero eigenvalue [24]. This allows us to rewrite Eq. (1) as

$$\mathbb{K}_n \cdot \boldsymbol{\pi} = \mathbf{e}_n, \quad (2a)$$

$$\mathbb{K}_n = \begin{matrix} 1 \\ \vdots \\ n-1 \\ n \\ n+1 \\ \vdots \\ N \end{matrix} \begin{pmatrix} W_{11} & W_{12} & \dots & W_{1N} \\ \vdots & \vdots & \dots & \vdots \\ W_{n-1,1} & W_{n-1,2} & \dots & W_{n-1,N} \\ 1 & 1 & \dots & 1 \\ W_{n+1,1} & W_{n+1,2} & \dots & W_{n+1,N} \\ \vdots & \vdots & \dots & \vdots \\ W_{N1} & W_{N2} & \dots & W_{N,N} \end{pmatrix}, \quad (2b)$$

where \mathbf{e}_n denotes the vector with a 1 for the n -th element and 0's elsewhere, and where the matrix \mathbb{K}_n coincides with the rate-matrix \mathbb{W} except the n -th row. Since the matrix \mathbb{K}_n is invertible [$\det \mathbb{K}_n \neq 0$] the solution of Eq. (2a) has the following form:

$$\boldsymbol{\pi} = \mathbb{K}_n^{-1} \cdot \mathbf{e}_n. \quad (3)$$

To find the linear response $\partial_\eta \boldsymbol{\pi}$ we calculate the derivative ∂_η of Eq. (2a):

$$\begin{aligned} \partial_\eta [\mathbb{K}_n(\eta) \cdot \boldsymbol{\pi}(\eta)] &= \mathbf{0}, \\ \mathbb{K}_n \cdot \partial_\eta \boldsymbol{\pi} &= -\partial_\eta \mathbb{K}_n \cdot \boldsymbol{\pi}. \end{aligned} \quad (4)$$

Solving Eq. (4), we arrive at the desired result:

$$\partial_\eta \boldsymbol{\pi} = -\mathbb{K}_n^{-1} \cdot \partial_\eta \mathbb{K}_n \cdot \boldsymbol{\pi}. \quad (5)$$

Equation (5) will be central in what follows. Indeed, it provides a linear algebra-based method to calculate different nonequilibrium responses which is much simpler and direct than methods based on graph theory representations of $\boldsymbol{\pi}$ [17]. At this stage, Eq. (5) holds for any dependence of $\mathbb{W}(\eta)$

* timur.aslyamov@uni.lu

† massimiliano.esposito@uni.lu

on the control parameter.

Rate-matrix model.—To proceed, we follow Ref. [17] and parameterize the nondiagonal elements of the rate matrix as

$$W_{ij} = e^{-(B_{ij}-E_j-F_{ij}/2)}, \quad (6)$$

where E_j are the vertex parameters, $B_{ij} = B_{ji}$ are the symmetric edge parameters, and $F_{ij} = -F_{ji}$ are the antisymmetric edge parameters. Expression (6) is reminiscent of Arrhenius rates that characterize the transition rates of a system in an energy landscape with wells of depths E_j , connected via barriers of heights B_{ij} , and subjected to nonconservative driving forces F_{ij} along the transition paths [17, 25]. These rates satisfy local detailed balance ensuring the compatibility with stochastic thermodynamics [25–27].

Vertex parameters.—To calculate $\partial_{E_n} \boldsymbol{\pi}$, we note that only the n -th column of the matrix \mathbb{K}_n depends on E_n . Therefore,

$$\partial_{E_n} \mathbb{K}_n = \begin{matrix} & & & & n \\ & & & & W_{1,n} \\ & & & & \vdots \\ & & & & W_{n-1,n} \\ \partial_{E_n} \mathbb{K}_n = & n & & & 0 \\ & n+1 & & & W_{n+1,n} \\ & & & & \vdots \\ & & & & W_{N,n} \\ & & & & \end{matrix} \quad (7)$$

where all columns but the n -th one are zero. The element (n, n) is zero because $K_{n,n} = 1$. Here and below, empty spaces in matrices denote zeros. Inserting Eq. (7) into Eq. (5), we immediately recover a key result of Ref. [17] obtained using nontrivial graph-theoretical methods, namely

$$\partial_{E_n} \boldsymbol{\pi} = -\pi_n \mathbb{K}_n^{-1} \cdot (\mathbf{K}_n - \mathbf{e}_n) = -\pi_n (\mathbf{e}_n - \boldsymbol{\pi}), \quad (8)$$

where \mathbf{K}_n is the n -th column of \mathbb{K}_n and where we used Eq. (3).

Symmetric edge parameters.—We proceed with calculating $\partial_{B_{nm}} \boldsymbol{\pi}$. One can see from Eq. (6) that such a perturbation changes W_{nm} and W_{mn} . These rates are also contained in the diagonal elements of the matrix \mathbb{W} since $W_{nn} = -\sum_{m \neq n} W_{mn}$. Overall four elements depend on B_{nm} : W_{nm} , W_{nn} , W_{mn} , W_{mm} . But the matrix \mathbb{K}_n defined in Eq. (2b) only contains two of those elements (due to row n). Using Eq. (6), their derivatives reads $\partial_{B_{nm}} W_{mn} = -W_{mn}$ and $\partial_{B_{nm}} W_{mm} = -\partial_{B_{nm}} W_{nm} = W_{nm}$, and we find that

$$\partial_{B_{nm}} \mathbb{K}_n = \begin{matrix} & & & & 1 \dots n \dots m \dots N \\ & & & & 1 \\ & & & & \vdots \\ & & & & -W_{mn} & W_{nm} \\ \partial_{B_{nm}} \mathbb{K}_n = & m & & & \\ & & & & \vdots \\ & & & & W_{nm} \\ & & & & N \end{matrix} \quad (9)$$

Calculating $(\partial_{B_{nm}} \mathbb{K}_n) \cdot \boldsymbol{\pi}$ and inserting into Eq. (5) we get:

$$\partial_{B_{nm}} \boldsymbol{\pi} = -\mathbb{K}_n^{-1} \cdot \mathbf{e}_m (W_{nm} \pi_m - W_{mn} \pi_n) = -\frac{\boldsymbol{\kappa}}{\det \mathbb{K}_n} J_{nm}, \quad (10)$$

where we recognize the NESS current $J_{nm} = W_{nm} \pi_m - W_{mn} \pi_n$ from m to n , and where $\boldsymbol{\kappa}/\det \mathbb{K}_n$ is the m -th column of the matrix \mathbb{K}_n^{-1} . The elements κ_i can be defined in terms of the minors $M_{im}(\mathbb{K}_n^T)$ of the matrix \mathbb{K}_n^T :

$$\kappa_i = (-1)^{i+m} M_{im}(\mathbb{K}_n^T) = (-1)^{i+m} M_{mi}(\mathbb{K}_n). \quad (11)$$

Since the minors $M_{mi}(\mathbb{K}_n)$ do not include the m -th row of the matrix \mathbb{K}_n , the elements κ_i do not depend on B_{nm} and F_{nm} [see Eq. (2b)].

Expression (10) is a new result. In Ref. [17], only the following bound was obtained: $|\partial_{B_{nm}} \pi_i| \leq \pi_i (1 - \pi_i) \tanh(F_{\max}/4)$, where F_{\max} is the maximum absolute value of the affinity along all cycles containing the edge (n, m) . A numerical comparison between the two is given in Appendix B, see Fig. 1. A direct implication of our result is that the response is suppressed, $\partial_{B_{nm}} \boldsymbol{\pi} = 0$, when the edge (n, m) is detailed balanced $J_{nm} = 0$. Instead, ensuring the suppression of the response from the bound [17], implies the more restrictive condition $F_{\max} = 0$, which corresponds to equilibrium where all edge currents vanish. An example where an edge current vanishes while the forces are non-zero is provided in Appendix B. They have also been shown to produce ‘‘Green-Kubo-like’’ FDR [9].

Antisymmetric edge parameters.—We now calculate $\partial_{F_{nm}} \boldsymbol{\pi}$ from Equation (5). The non-zero elements of $\partial_{F_{nm}} \mathbb{K}_n$ are $\partial_{F_{nm}} W_{mn} = -W_{mn}/2$ and $\partial_{F_{nm}} W_{mm} = -\partial_{F_{nm}} W_{nm} = -W_{nm}/2$:

$$\partial_{F_{nm}} \mathbb{K}_n = \begin{matrix} & & & & 1 \dots n \dots m \dots N \\ & & & & 1 \\ & & & & \vdots \\ & & & & -W_{mn}/2 & -W_{nm}/2 \\ \partial_{F_{nm}} \mathbb{K}_n = & m & & & \\ & & & & \vdots \\ & & & & W_{nm} \\ & & & & N \end{matrix} \quad (12)$$

Using Eq. (5), we arrive at:

$$\partial_{F_{nm}} \boldsymbol{\pi} = \mathbb{K}_n^{-1} \cdot \mathbf{e}_m \frac{W_{nm} \pi_m + W_{mn} \pi_n}{2} = \frac{\boldsymbol{\kappa}}{\det \mathbb{K}_n} \frac{\tau_{nm}}{2}, \quad (13)$$

where $\tau_{nm} = W_{nm} \pi_m + W_{mn} \pi_n$ is the edge traffic (related to the expected escape rate, activity and frenesy [28]). In Ref. [17], only the following bound was obtained $|\partial_{F_{nm}} \pi_i| \leq \pi_i (1 - \pi_i)$.

Responses of current and traffic.—Using Eqs. (10) and (13), the sensitivities of the edge currents reads:

$$\partial_{B_{nm}} \ln J_{nm} = -1 + \Delta_{nm}, \quad (14a)$$

$$\partial_{F_{nm}} \ln J_{nm} = \frac{\tau_{nm} (1 - \Delta_{nm})}{J_{nm} 2}, \quad (14b)$$

$$\Delta_{nm} = \frac{W_{mn} \kappa_n - W_{nm} \kappa_m}{\det \mathbb{K}_n}. \quad (14c)$$

Similarly, the sensitivities of edge traffic reads:

$$\partial_{B_{nm}} \ln \tau_{nm} = -1 - \frac{J_{nm}}{\tau_{nm}} \nabla_{nm}, \quad (15a)$$

$$\partial_{F_{nm}} \ln \tau_{nm} = \frac{1}{2} \left(\frac{J_{nm}}{\tau_{nm}} + \nabla_{nm} \right), \quad (15b)$$

$$\nabla_{nm} = \frac{W_{mn}\kappa_n + W_{nm}\kappa_m}{\det \mathbb{K}_n}. \quad (15c)$$

These two results, Eqs. (14) and (15), are important because they provide explicit algebraic expressions for the response. Indeed, the variables Δ_{nm} and ∇_{nm} defined in Eqs. (14c) and (15c) do not depend on π_i . They depend only on the elements in the minors (m, n) and (m, m) of the matrix \mathbb{K}_n .

control	current, J_{nm}	traffic, τ_{nm}
B_{nm}	$-1 \leq \frac{\partial \ln J_{nm}}{\partial B_{nm}} \leq 0$	$-2 \leq \frac{\partial \ln \tau_{nm}}{\partial B_{nm}} \leq 0$
F_{nm}	$0 \leq \frac{2}{\tau_{nm}} \frac{\partial J_{nm}}{\partial F_{nm}} \leq 1$	$-1 \leq \frac{\partial \ln \tau_{nm}}{\partial F_{nm}} \leq 1$

TABLE I. The central and right columns correspond to the response of the current and traffic, respectively. The central and bottom rows are perturbations of the symmetric and antisymmetric edge parameters, respectively.

Bounds and discussion.—Another important result is that simple bounds can be obtained for Eqs. (14) and (15). They are given in Table I and bound the sensitivities $\partial_\eta \ln q$ for all combinations of $q = \{J_{nm}, \tau_{nm}\}$ and $\eta = \{B_{nm}, F_{nm}\}$. In Appendix A, we derive the following bounds for Δ_{nm} and ∇_{nm} ,

$$0 \leq \Delta_{nm} \leq 1, \quad (16a)$$

$$|\nabla_{nm}| \leq \Delta_{nm} \leq 1, \quad (16b)$$

which can be used to prove all bounds in Table I. Indeed, inserting Eq. (16a) into Eqs. (14a) and (14b) we get two tight bounds for the current J_{nm} in Table I. Using Eqs. (15a), (15b), and (16b), we derive two tight bounds for the traffic

$$\left| \frac{\tau_{nm}}{J_{nm}} \left(\frac{\partial \ln \tau_{nm}}{\partial B_{nm}} + 1 \right) \right| \leq 1, \quad (17a)$$

$$\left| \frac{2 \partial \ln \tau_{nm}}{\partial F_{nm}} - \frac{J_{nm}}{\tau_{nm}} \right| \leq 1. \quad (17b)$$

The simpler bounds for τ_{nm} shown in Table I are not tight anymore. They are obtained using Eq. (16b) and $|J_{nm}/\tau_{nm}| \leq 1$ in Eqs. (15a) and (15b). To discuss the saturation of the tight bounds in Table I and Eq. (17), we consider one of them:

$$-1 \leq \partial_{B_{nm}} \ln J_{nm} \leq 0. \quad (18)$$

The upper bound in Eq. (18) is simple to understand: a higher

energy barrier (B_{nm}) always results in a lower absolute value of the current between states n and m . This bound is saturated at $\Delta_{nm} = 1$, which reveals another (topological) way to reduce the response of the current. To saturate the lower bound in Eq. (18), one needs $\Delta_{nm} = 0$. However, in Appendix A we prove that $\Delta_{nm} = 0$ only if $W_{nm} = W_{mn} = 0$ or $\kappa_m = \kappa_n = 0$, where the former condition is equivalent to $J_{nm} = 0$. Therefore, excluding the case $\kappa_m = \kappa_n = 0$, the lower bound of Eq. (18) can be saturated only for a zero current. This is illustrated by the numerical simulations shown in Fig. 2, where the set of possible values $\partial_{B_{nm}} \ln J_{nm}$ touches the edge -1 only at one point $J_{nm} = 0$. The bound for the sensitivity $\partial_{F_{nm}} \ln J_{nm}$ has the same properties as Eq. (18). The bounds in Eq. (17) saturate at $\nabla_{nm} = \pm 1$, which implies $\Delta_{nm} = 1$, see Eq. (16b).

Future studies.—Our first main result Eq. (5) provides a general algebraic expression of a NESS response with respect to any parameterization of the rate matrix. Our other results rely on the Arrhenius-like form (6) of the rates, which allows us to perturb isolated edges. But our methodology can be extended to consider more general rate matrices with nonconservative force acting on multiple edges [16, 26, 29]. It could also be used to study the stationary responses of other physical observables (beyond currents and activities) [30, 31], as well as to study time-dependent ‘‘Green-Kubo-Agarwal-like’’ relations [7, 11].

Acknowledgments.—This research was funded by project ChemComplex (C21/MS/16356329). We thank Massimo Bilancioni for detailed feedback on our manuscript.

Appendix A: Proof of bounds in Eq. (16)

We prove the bounds in Eq. (16). The determinant $\det \mathbb{K}_n$ on the m -th row of the matrix \mathbb{K}_n can be written as

$$\begin{aligned} \det \mathbb{K}_n &= (-1)^{m+n} W_{mn} M_{mn}(\mathbb{K}_n) + (-1)^{m+m} W_{mm} M_{mm}(\mathbb{K}_n) \\ &\quad + \sum_{i \neq m, n} (-1)^{i+m} W_{mi} M_{mi}(\mathbb{K}_n) \\ &= W_{mn} \kappa_n - W_{nm} \kappa_m + C, \end{aligned} \quad (A1)$$

where we used Eq. (11) and where C denotes the sum of all terms which do not depend on B_{nm} and F_{nm} . Since $\det \mathbb{K}_n = \prod_i^{N-1} \lambda_i$, where λ_i are nonzero negative eigenvalues of the matrix \mathbb{W} (see [32]), the sign of the determinant $\text{sgn} \det \mathbb{K}_n = (-1)^{N-1}$ is fixed and does not depend on B_{nm} and F_{nm} . Using the fact that C does not depend on B_{nm} , we can determine the sign of C from Eq. (A1) in the limit $B_{nm} \rightarrow \infty$, where $W_{nm}, W_{mn} \rightarrow 0$:

$$\text{sgn} C = \lim_{B_{nm} \rightarrow \infty} \text{sgn} \det \mathbb{K}_n = (-1)^{N-1}. \quad (A2)$$

Using the fact that the signs of C and $\det \mathbb{K}_n$ are the same, we can rewrite Eq. (14c) using Eq. (A1) as

$$\Delta_{nm} = 1 - \left| \frac{C}{\det \mathbb{K}_n} \right|, \quad (A3)$$

which gives us the upper bound in Eq. (16a).

In the case $\kappa_n = 0, \kappa_m = 0$, Eqs. (14c) and (15c) satisfy the bounds (16a) and (16b). Considering $\kappa_n \neq 0$ and $\kappa_m \neq 0$, the following limits of Eq. (A1) hold:

$$\lim_{B_{nm} \rightarrow -\infty} \det \mathbb{K}_n = W_{mn}\kappa_n - W_{nm}\kappa_m, \quad (\text{A4a})$$

$$\lim_{F_{nm} \rightarrow \infty} \det \mathbb{K}_n = -W_{nm}\kappa_m, \quad (\text{A4b})$$

$$\lim_{F_{nm} \rightarrow -\infty} \det \mathbb{K}_n = W_{mn}\kappa_n. \quad (\text{A4c})$$

Since $\text{sgn}(W_{mn}\kappa_n/\det \mathbb{K}_n)$ and $\text{sgn}(W_{nm}\kappa_m/\det \mathbb{K}_n)$ are fixed, we can find them using Eqs. (A4b) and (A4c)

$$\text{sgn}\left(\frac{W_{mn}\kappa_n}{\det \mathbb{K}_n}\right) = \lim_{F_{nm} \rightarrow -\infty} \frac{W_{mn}\kappa_n}{\det \mathbb{K}_n} = 1, \quad (\text{A5a})$$

$$\text{sgn}\left(\frac{W_{nm}\kappa_m}{\det \mathbb{K}_n}\right) = \lim_{F_{nm} \rightarrow \infty} \frac{W_{nm}\kappa_m}{\det \mathbb{K}_n} = -1, \quad (\text{A5b})$$

which implies the lower bound in Eq. (16a) and

$$\kappa_n \kappa_m < 0. \quad (\text{A6})$$

Combining Eqs. (A3) and (A5), we derive the inequalities (16a).

The lower bound in Eq. (16a) is saturated only when $W_{nm} = W_{mn} = 0$, while for $W_{nm} \neq 0$ the condition in Eq. (A6) implies $\Delta_{nm} \neq 0$. The upper bound in Eq. (16a) is saturated in the limit $B_{nm} \rightarrow -\infty$ [see Eqs. (14c) and (A4a)], as well as when $C = 0$.

To find bounds for ∇_{nm} , we rewrite it as follows:

$$\nabla_{nm} = \Delta_{nm} \frac{W_{mn}\kappa_n + W_{nm}\kappa_m}{W_{mn}\kappa_n - W_{nm}\kappa_m}. \quad (\text{A7})$$

If $W_{mn}\kappa_n = 0$, then $\nabla_{nm} = -\Delta_{nm}$, otherwise we have:

$$\nabla_{nm} = \Delta_{nm} \frac{1+a}{1-a}, \quad \text{where } a = \frac{W_{nm}\kappa_m}{W_{mn}\kappa_n} \leq 0. \quad (\text{A8})$$

Since $|(1+a)/(1-a)| \leq 1$ for $a \leq 0$, we find Eq. (16b).

In the case $\kappa_n = 0, \kappa_m \neq 0$ (resp. $\kappa_n \neq 0, \kappa_m = 0$), we derive Eq. (16a) using Eq. (A3) and Eq. (A5b) (resp. Eq. (A5a)); and we have $\nabla_{nm} = -\Delta_{nm}$ (resp. $\nabla_{nm} = \Delta_{nm}$).

Appendix B: Example of network

In Fig. 1, we consider the responses $\partial_{B_{13}}\pi_i$ with $i = 1, \dots, 4$, for the network given in the inset, and compare it to the bound $|\partial_{B_{13}}\pi_i| \leq \pi_i(1-\pi_i)\tanh(F_{\max}/4)$ obtained in [17]. We see that J_{13} can vanish even at nonzero value $F_{\max} = \max(|F_1|, |F_2|) \neq 0$. In other words, the system is out-of-equilibrium but the edge 1-3 is detailed balanced.

Appendix C: Numerical simulations

In Fig. 2, we numerically verify the bounds in Table I and Eq. (17) using random generated rate matrices for the net-

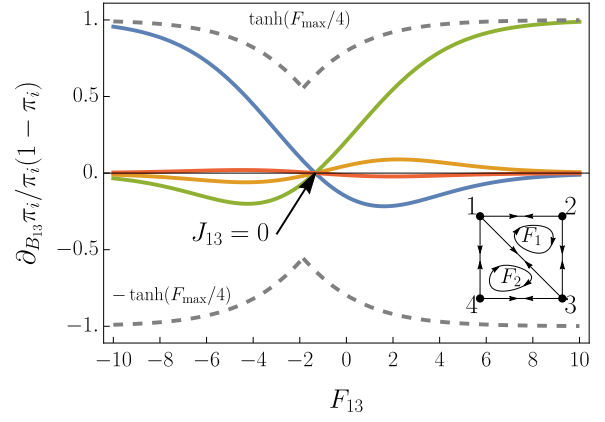


FIG. 1. Inset: Example of the network with 4 states; F_1 and F_2 denote the forces in the cycles 1-2-3-1 and 1-4-3-1, respectively. Main: The solid curves show the responses $\partial_{B_{13}}\pi_i$ from Eq. (10) scaled by $\pi_i(1-\pi_i)$, where $i = 1, 2, 3, 4$ correspond to blue, orange, green, and red colors, respectively. In these coordinates, the dashed lines ($\pm \tanh(F_{\max}/4)$) correspond to the bound from [17]. Black arrow indicates $J_{13} = 0$. Simulation parameters: the nondiagonal and nonzero elements of \mathbb{W} are $W_{21} = 10.8$, $W_{31} = 13.4e^{-B_{13}-F_{13}/2}$, $W_{41} = 16.2$, $W_{12} = 94.8$, $W_{32} = 26.6$, $W_{13} = 45.5e^{-B_{13}+F_{13}/2}$, $W_{23} = 19.5$, $W_{43} = 14.3$, $W_{14} = 0.5$, $W_{34} = 9.8$, where $B_{13} = 1$. The forces in the inset are $F_1 = F_{13} - 0.6$, $F_2 = F_{13} + 4.4$ which give $|F_1| = |F_2|$ at $F_{13} = -1.9$.

work shown in the inset of Fig. 1.

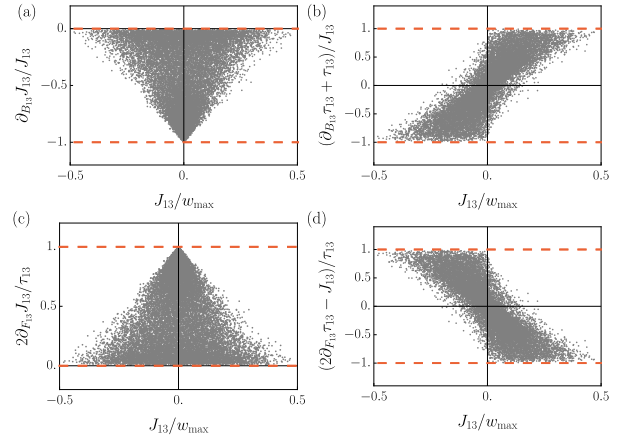


FIG. 2. a-d: Illustrations of the bounds of J_{nm} from Table I and τ_{nm} from Eq. (17). The dashed lines show the corresponding bounds. The dots are the result of numerical calculations for 20000 random matrices \mathbb{W} with a homogeneous distribution of elements in the range $(0, w_{\max})$. The network corresponds to the inset in Fig. 1, $w_{\max} = 100$.

-
- [1] U. M. B. Marconi, A. Puglisi, L. Rondoni, and A. Vulpiani, *Physics reports* **461**, 111 (2008).
- [2] M. Polettni and M. Esposito, *Journal of Statistical Physics* **176**, 94 (2019).
- [3] J. A. Owen and J. M. Horowitz, *Nature Communications* **14**, 1280 (2023).
- [4] R. Kubo, *Reports on progress in physics* **29**, 255 (1966).
- [5] D. Forastiere, R. Rao, and M. Esposito, *New Journal of Physics* **24**, 083021 (2022).
- [6] G. S. Agarwal, *Zeitschrift für Physik A Hadrons and nuclei* **252**, 25 (1972).
- [7] U. Seifert and T. Speck, *Europhysics Letters* **89**, 10007 (2010).
- [8] J. Prost, J.-F. Joanny, and J. M. Parrondo, *Physical review letters* **103**, 090601 (2009).
- [9] B. Altaner, M. Polettni, and M. Esposito, *Physical review letters* **117**, 180601 (2016).
- [10] M. Baiesi, C. Maes, and B. Wynants, *Physical review letters* **103**, 010602 (2009).
- [11] M. Baiesi and C. Maes, *New Journal of Physics* **15**, 013004 (2013).
- [12] M. Baldovin, L. Caprini, A. Puglisi, A. Sarracino, and A. Vulpiani, in *Nonequilibrium Thermodynamics and Fluctuation Kinetics: Modern Trends and Open Questions* (Springer, 2022) pp. 29–57.
- [13] T. Hatano and S.-i. Sasa, *Physical review letters* **86**, 3463 (2001).
- [14] G. Falasco, T. Cossetto, E. Penocchio, and M. Esposito, *New Journal of Physics* **21**, 073005 (2019).
- [15] N. Shiraishi, *Physical Review Letters* **129**, 020602 (2022).
- [16] A. Dechant and S.-i. Sasa, *Proceedings of the National Academy of Sciences* **117**, 6430 (2020).
- [17] J. A. Owen, T. R. Gingrich, and J. M. Horowitz, *Physical Review X* **10**, 011066 (2020).
- [18] E. L. King and C. Altman, *The Journal of physical chemistry* **60**, 1375 (1956).
- [19] T. L. Hill, *Journal of theoretical biology* **10**, 442 (1966).
- [20] J. Schnakenberg, *Reviews of Modern physics* **48**, 571 (1976).
- [21] A. C. Barato and U. Seifert, *Physical review letters* **114**, 158101 (2015).
- [22] T. R. Gingrich, J. M. Horowitz, N. Perunov, and J. L. England, *Physical review letters* **116**, 120601 (2016).
- [23] G. Falasco and M. Esposito, *Physical Review Letters* **125**, 120604 (2020).
- [24] N. G. Van Kampen, *Stochastic processes in physics and chemistry*, Vol. 1 (Elsevier, 1992).
- [25] G. Falasco and M. Esposito, *Physical Review E* **103**, 042114 (2021).
- [26] R. Rao and M. Esposito, *New Journal of Physics* **20**, 023007 (2018).
- [27] C. Maes, *SciPost Physics Lecture Notes*, 032 (2021).
- [28] C. Maes, *Physics Reports* **850**, 1 (2020).
- [29] G. Falasco and M. Esposito, *Macroscopic stochastic thermodynamics* (2023), [arXiv:2307.12406 \[cond-mat.stat-mech\]](https://arxiv.org/abs/2307.12406).
- [30] G. F. Martins and J. M. Horowitz, *arXiv preprint arXiv:2305.19348* <https://doi.org/10.48550/arXiv.2305.19348> (2023).
- [31] H.-M. Chun and J. M. Horowitz, *The Journal of Chemical Physics* **158**, <https://doi.org/10.1063/5.0148662> (2023).
- [32] We use Theorem 2 from page 157 of Ref. [33] to write $\det \mathbb{K}_n = (-1)^{N-1} \lim_{\lambda \rightarrow 0} \det(\lambda \mathbb{E} - \mathbb{W})/\lambda = (-1)^{N-1} \prod_{i=1}^{N-1} (-\lambda_i)$.
- [33] P. Lancaster and M. Tismenetsky, *The Theory of Matrices: With Applications*, Computer Science and Scientific (Academic Press, 1985).